A rare variant in *Anp32B* impairs influenza virus replication in human cells

Ecco Staller, Laury Baillon, Rebecca Frise, Thomas P. Peacock, Carol M. Sheppard, Vanessa Sancho-Shimizu, and Wendy Barclay*

Department of Infectious Disease, Faculty of Medicine, Imperial College London, United Kingdom

*Corresponding author: w.barclay@imperial.ac.uk

SUMMARY

Viruses require host factors to support their replication, and genetic variation in such factors can affect susceptibility to infectious disease. Influenza virus replication in human cells relies on ANP32 proteins, which serve essential but redundant roles to support influenza virus polymerase activity. Here, we investigate naturally occurring single nucleotide variants (SNV) in the human *Anp32A* and *Anp32B* genes. We note that variant rs182096718 in *Anp32B* is found at a higher frequency than other variants in either gene. This variant results in a D130A substitution in ANP32B, which is less able to support influenza virus polymerase (FluPol) activity than wildtype ANP32B. Using a split luciferase binding assay, we also show reduced interaction between ANP32B-D130A and FluPol. We then use CRISPR/Cas9 genome editing to generate the mutant homozygous genotype in human eHAP cells, and show that FluPol activity and virus replication are attenuated in cells expressing wildtype ANP32A and mutant ANP32B-D130A. This is in contrast to cells that completely lack expression of ANP32B where no attenuation is seen. We conclude that ANP32B-D130A exerts a dominant negative effect on the pro-viral activity of ANP32A in cells, and suggest that carriers of rs182096718 may have some genetic protection against influenza viruses.

KEYWORDS

Influenza virus, ANP32B, mutation, single nucleotide variant, host factor

INTRODUCTION

All viruses rely on host factors to support their replication. Genetic variation in such proteins can affect susceptibility to infectious disease (Ciancanelli et al., 2016; Karlsson et al., 2014; Pittman et al., 2016; Zhang, 2020). Perhaps the best-known mutation conferring innate genetic resistance to viral infection is the Δ32 variant of the HIV-1 co-receptor C-C chemokine receptor type 5 (*CCR5*) (Carrington et al., 1999). Single nucleotide variants that reduce susceptibility to virus infection include a P424A substitution in the filovirus endosomal fusion receptor Niemann-PickC1 (*NPC1*) (Carette et al., 2011; Kondoh et al., 2018), and a G428A mutation in fucosyltransferase 2 (*FUT2*) that renders homozygous carriers resistant to norovirus (Lindesmith et al., 2003; Thorven et al., 2005). A mutation in interferon-induced transmembrane protein 3 (*IFITM3*) has been associated with increased severity of infection with influenza virus (Ciancanelli et al., 2016; Everitt et al., 2012; Prabhu et al., 2018; Zhang et al., 2013), as have monogenic lesions of *GATA2*, *IRF7*, *IRF9* and *TLR3* (Zhang, 2020). Besides a pair of polymorphisms in the non-coding region (NCR) of *LGALS1*, which may confer some protection from H7N9 influenza A virus (IAV) in Chinese poultry workers (Chen et al., 2015), no single nucleotide variants protective against influenza virus have thus far been described.

Influenza replication and transcription are carried out in the host cell nucleus by the virus-encoded heterotrimeric RNA-dependent RNA polymerase (Te Velthuis and Fodor, 2016), which relies on host factors to support RNA synthesis (Peacock et al., 2019). Influenza

viruses co-opt the host proteins acidic nuclear phosphoprotein 32 kilodaltons A (ANP32A) and ANP32B to support their replication (Long et al., 2016; Staller et al., 2019; Zhang et al., 2019). ANP32A and ANP32B are functionally redundant in their support for influenza virus: in human cells lacking either but not both ANP32A (AKO) or ANP32B (BKO), virus proliferation is not impaired. In cells lacking both proteins (dKO), however, FluPol activity and virus growth are completely abrogated (Staller et al., 2019; Zhang et al., 2019). ANP32 proteins are expressed in many different human tissues, including fibroblasts and lung (Lonsdale et al., 2013), and involved in a wide range of cellular processes, including apoptosis and transcriptional regulation (Reilly et al., 2014). ANP32A and ANP32B are 249 and 251 amino acids long, respectively, with two major domains: a structured N-terminal leucine-rich repeat region (LRR) and an unresolved low-complexity acidic region (LCAR) (Huyton and Wolberger, 2007; Tochio et al., 2010). Mutational analysis of ANP32 proteins of several species relevant to influenza has shown that the identity of amino acid residues 129 and 130 dictates pro-viral function (Long et al., 2019; Peacock et al., 2020; Staller et al., 2019; Zhang et al., 2019). ANP32 proteins that cannot be co-opted by influenza virus include human ANP32E (unpublished data), chicken ANP32B, and mouse ANP32A. What these orthologues have in common is divergence from the pro-viral dyad 129N-130D: human ANP32E has glutamate at position 129 (129E) rather than asparagine, chicken ANP32B has isoleucine at position 129 (129I) and asparagine at position 130 (130N), and mouse ANP32A has alanine at position 130 (130A), suggesting that these amino acids are important for pro-viral activity of ANP32 proteins.

Here we describe natural variation in the human *Anp32A* and *Anp32B* genes, in particular the relatively enriched SNV rs182096718 in *Anp32B,* which has a global minor allele frequency (MAF) of 0.0044 and is prevalent in 3.41% of individuals of Hispanic / Latino ethnicity. SNV rs182096718 translates to a mutant ANP32B-D130A protein product, and is the only variant for which homozygous carriers exist. We generated the homozygous mutant genotype (wildtype *Anp32A* / mutant *Anp32B*) in low-ploidy human eHAP cells (Essletzbichler et al., 2014) by CRISPR/Cas9 genome editing. Using minigenome reporter assays and virus challenge, we found that IAV FluPol activity and replication were severely restricted in monoclonal cells expressing wildtype ANP32A and ANP32B-D130A. We conclude that cells expressing ANP32B-D130A alongside wildtype ANP32A are less able to support influenza polymerase activity, even when compared with cells that lack ANP32B expression (BKO). This suggests a potential dominant negative effect of ANP32B-D130A on ANP32A pro-viral activity. We speculate that carriers of this variant may have some resistance to influenza viruses.

RESULTS

A relatively common variant encodes ANP32B-D130A

We searched public databases for rare missense SNVs in the human *Anp32A* and *Anp32B* genes that were predicted, on the basis of our previous work, to have functional impact on the pro-influenza virus activity of the proteins. The databases included the dbSNP from the National Center for Biotechnology Information (NCBI) (Sherry et al., 2001), the Avon Longitudinal Study of Parents and Children (ALSPAC) (Walter et al., 2015), Trans-Omics for Precision Medicine (TOPMed) (Taliun et al., 2019), the 1000 Genomes Project (Genomes Project et al., 2015), the Grand Opportunity Exome sequencing Project (GO-ESP) (Fu et al., 2013), and the genome aggregation database (gnomAD) (Karczewski et al., 2019). The latter lists a total 54 missense SNVs in *Anp32A* and 82 in *Anp32B.*

Four SNVs in *Anp32A* and five in *Anp32B* were selected for investigation, taking into account changes in charge, bulk, polarity and putative solvent exposure of the encoded

amino acid substitutions (Huyton and Wolberger, 2007; Tochio et al., 2010), as well as the previously established importance of positions 129 and 130 for pro-influenza viral activity (Figure 1A). All the variants in *Anp32A* are exceedingly rare (MAF<0.001), and no homozygous carriers have been identified. The serine mutants at position 158 were selected as this is a putative phosphorylation site (Hong et al., 2004). The SNV responsible for a mutant ANP32A-D130N protein (rs771143708) is found in a single heterozygous individual out of 3,854 in the ALSPAC cohort, rs751239680 (ANP32A-R132Q) is found in a single heterozygous individual out of 10,052 in the African cohort of the gnomAD database, rs772530468 (ANP32A-S158T) is present in a single South Asian male in 23,070 in the gnomAD database, as well as two separate homozygous individuals in the TOPMed database. Finally, a single African male in 5,032 in the gnomAD database is a heterozygous carrier of rs772530468 (ANP32A-S158A) (Figure 1B).

Most variants in *Anp32B* were also low-frequency (MAF<0.0001): rs377406514 (ANP32B-L128V) is found in a single African female out of 10,066 in the gnomAD database; rs771977254 (ANP32B-E133Q) occurs in two out of 4,900 Ashkenazi Jewish females in the gnomAD database; rs761932651 (ANP32B-L138H) is found in one South Asian male in 23,070 in the gnomAD database; rs770020996 (ANP32B-L142F) occurs in one female in 7,544 and one male in 23,072 from the South Asian cohort of the gnomAD database (Figure 1C). There is, however, an exception. SNV rs182096718, encoding ANP32B-D130A, is relatively common in the Hispanic / Latino cohort of the gnomAD database, where in a total pool of 35,420 alleles 1,209 minority alleles were identified, as well as 25 homozygous carriers. The D130A substitution in ANP32B is thus present in 3.41% of the Latino cohort, which, compared with all other SNVs in either *Anp32A* or *Anp32B* is a relatively high frequency. We and others have previously shown that murine ANP32A, which naturally harbours 130A, does not support influenza virus polymerase. Substituting 130A in human ANP32A greatly reduced FluPol activity, while introducing 130D in mouse ANP32A rescued its capacity to support FluPol activity (Staller et al., 2019; Zhang et al., 2019). Indeed, ANP32B KO mice, but not ANP32A KO mice, showed reduced viral loads and mortality when infected with H3N2 or H5N1 influenza A virus (Beck et al., 2020).

A

Gene	ID	Variant	Amino acid substitution	Minor allele frequency	Source	Heterozygous carriers	Homozygous carriers
Anp32A	rs771143708	C>T	D130N	T=0.0003	ALSPAC	1	0
	rs751239680	C>T	R132Q	T<0.0001	ExAC	1	0
	rs772530468	A>C	S158T	C<0.0001	gnomAD TOPMed	3	0
		A>T	S158A	T<0.0001	ExAC gnomAD	1	0
Anp32B	rs377406514	C>G	L128V	G<0.0001	gnomAD	1	0
	rs182096718	A>C	D130A	C=0.0044	gnomAD 1000G GO-ESP TOPMed	1,233	25
	rs771977254	G>C	E133Q	C<0.0001	gnomAD	2	0
	rs761932651	T>A	L138H	A<0.0001	gnomAD	1	0
	rs770020996	C>T	L142F	T<0.0001	gnomAD	2	0

B

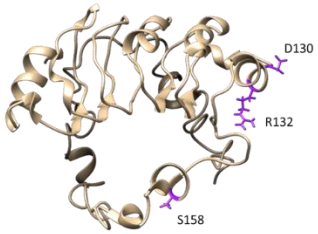

C

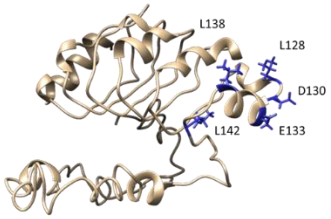

Figure 1. Selected naturally occurring missense single nucleotide variants in Anp32A and Anp32B *(A) NCBI dbSNP Reference IDs, variant, amino acid substitution, global minor allele frequency (MAF), source database, and number of heterozygous and homozygous carriers for each*

variant (B) Structural model of ANP32A showing amino acids affected by selected SNVs (C) Structural model of ANP32B showing amino acids affected by selected SNVs

Selected mutant ANP32 proteins affect FluPol activity

The capacity of each mutant protein, when expressed exogenously in human eHAP cells lacking ANP32A and ANP32B (dKO), to support reconstituted polymerases from a seasonal H3N2 virus (A/Victoria/3/75) and a 2009 pandemic H1N1 isolate (A/England/195/2009) was tested in minigenome reporter assays (Figure 2). ANP32A-D130N did not support IAV polymerase, while R132Q and S158A substitutions were significantly reduced in their capacity to support FluPol activity. ANP32A-S158T, in contrast, supported FluPol to an extent similar to wildtype ANP32A (Figure 2A and B). ANP32B-D130A had a large deleterious effect on the support for FluPol activity, as did the leucine to valine substitution at position 128 (ANP32B-L128V). ANP32B-E133Q was also significantly less able to support FluPol activity. Substitutions of the leucines at positions 138 and 142 to histidine (L138H) and phenylalanine (L142F), respectively, did not reduce the ability of the mutant ANP32B proteins to support FluPol activity (Figure 2D and E). None of the differences were explained by changes in expression (Figure 2C and F) or nuclear localisation of the mutant proteins (Supplementary Figure 1).

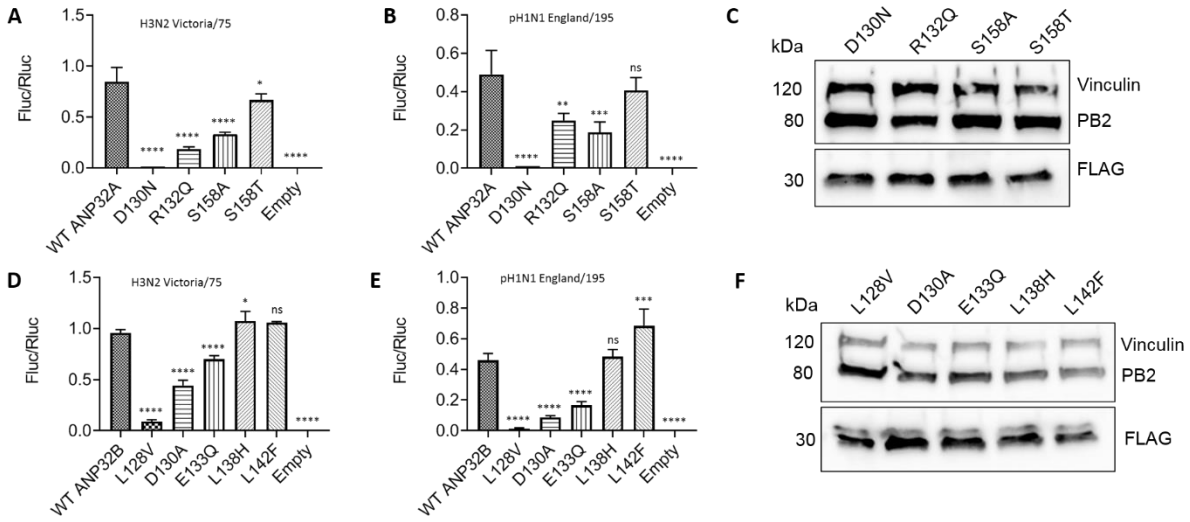

Figure 2 ANP32A and B mutant proteins show variable capacity to rescue IAV FluPol activity *(A) and (B) Minigenome reporter assays in eHAP dKO cells with co-transfected FLAG-tagged ANP32A variants with H3N2 Victoria (A) or pH1N1 Eng/195 (B) RNP components (PB1, PB2, PA and NP), pPolI-firefly luciferase minigenome reporter, and Renilla luciferase control. Data show mean (SD) of firefly activity normalized to Renilla and analysed by one-way ANOVA from one representative repeat (n = 2 independent triplicate experiments). Panels (D) and (E) show identical experiments with ANP32B constructs. ns, not significant; *, P < 0.05; **, P < 0.01; ***, P < 0.001; ****, P < 0.0001. (C) and (F) Western blotting analysis showing expression of H3N2 Victoria PB2 and FLAG tagged mutant ANP32A (C) or ANP32B (F) constructs compared with Vinculin loading control. Blots are representative of minigenome assays shown in (A) and (D), respectively.*

Using a split luciferase complementation assay previously developed in our laboratory (Cassonnet et al., 2011; Mistry et al., 2020) (Figure 3A) we next assessed whether the

ANP32 mutants whose pro-viral function was most impaired (ANP32A-D130N, ANP32B-L128V, and ANP32B-D130A) showed reduced binding to FluPol. The luciferase signal indicating binding of ANP32A-D130N to FluPol was reduced >7-fold, relative to wildtype ANP32A (Figure 3B). FluPol interactions of ANP32B-L128V and ANP32B-D130A were also reduced, resulting in luciferase signals of around half those measured with the wildtype ANP32B (Figure 3C). The poor pro-viral function of these mutants is thus, at least in part, explained by reduced interaction with trimeric influenza polymerase. Interestingly, binding of mouse ANP32A to Vic/75 H3N2 FluPol was reduced 2.5-fold compared with mouse ANP32B, and 3.2-fold compared with human ANP32A (Figure 3D)

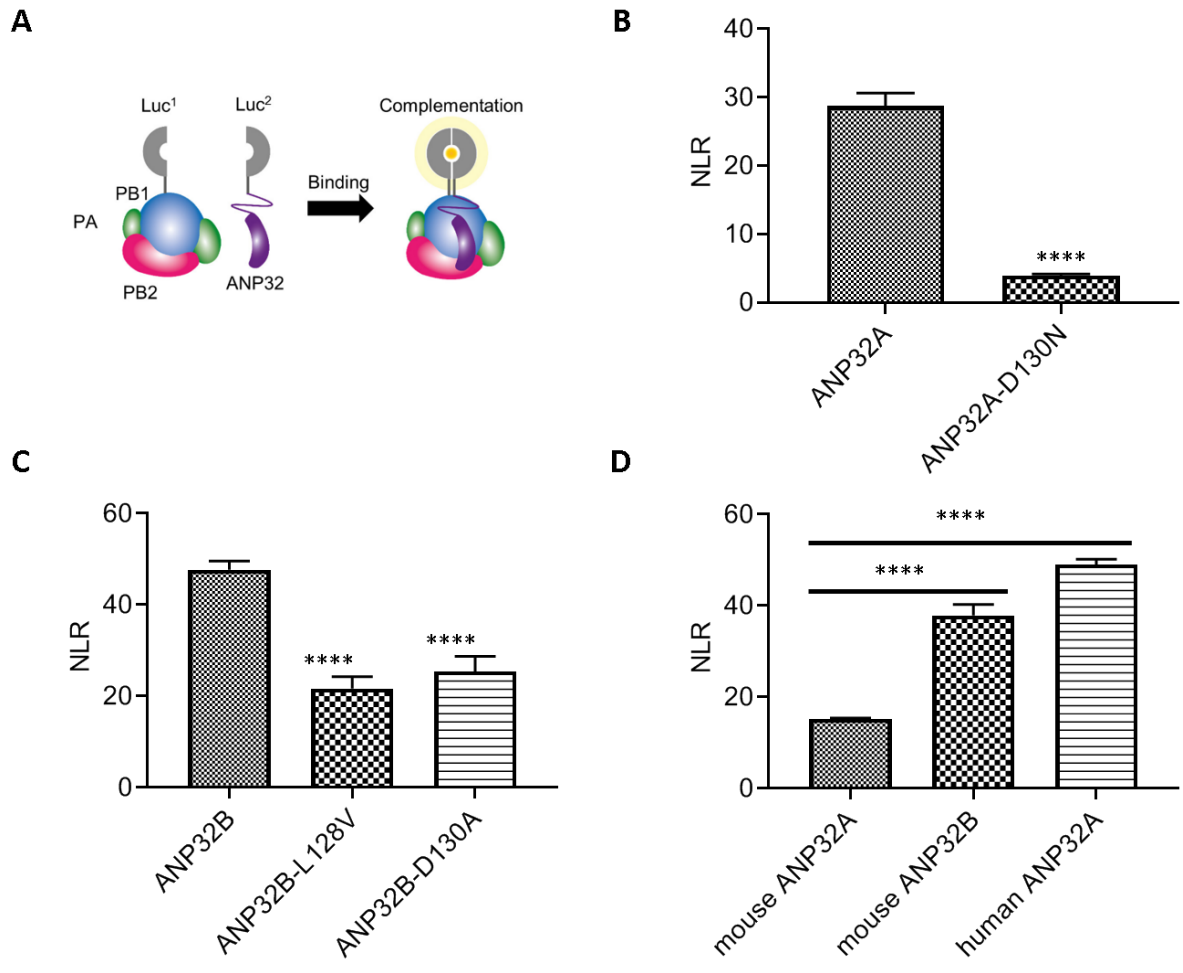

Figure 3 Poor pro-viral function of ANP32 mutants correlates with poor binding to FluPol *(A) Schematic of split luciferase complementation assay (adapted from Mistry et al. 2019) (B-D) Equal amounts (15 ng) of pCAGGS expression plasmids encoding H5N1 50-92 polymerase or H3N2 Vic/75 components (PB1-luc1, PB2-627K and PA), as well as ANP32-luc2, were transfected into 293T cells. 24 hours post-transfection cells were lysed and luminescence was measured. Two separate sets of control wells were transfected with either untagged PB1, PB2-627K, PA, ANP32-luc2 and unbound luc1, or untagged ANP32, PB1-luc1, PB2-627K, PA and unbound luc2. Total amount of plasmid (in ng) was kept constant by using empty pCAGGS. Normalised luminescence ratio (NLR) was obtained by dividing luminescence in the experimental condition (tagged PB1 + tagged ANP32) by the sum of the luminescence measured in the control conditions (i.e. background interaction of unbound luc1 with ANP32-luc2, and unbound luc2 with PB1-luc1, respectively). (B) Interaction between ANP32A-D130N mutant and H5N1 50-92 FluPol, compared with wildtype ANP32A (C) Interactions between ANP32B-L128V and ANP32B-D130A mutants and H5N1 50-92 FluPol, compared with wildtype ANP32B. (D)*

*Interaction between mouse ANP32A and Vic/75 FluPol compared with mouse ANP32B and human ANP32A. Data shown are mean (SD) representative of two independent triplicate experiments; statistical analysis in (B) by Student t-test, in (C and D~~?~~) by one-way ANOVA. ****, P < 0.0001*

As ANP32B-D130A is by far the most common SNV, and homozygous carriers of this variant exist, we focused our further efforts on this mutant. Although ANP32A and ANP32B are functionally redundant in their pro-viral activity, we reasoned the SNV might confer a phenotype if it exerted a dominant negative effect over wildtype ANP32A. To test this we titrated increasing concentrations of either wildtype ANP32B or ANP32B-D130A in dKO cells, alongside a constant amount of wildtype ANP32A (Supplementary Figure 2). Overexpressing ANP32B-D130A in the presence of wildtype ANP32A in dKO cells resulted in decreased FluPol activity. This effect was not seen when co-expressing wildtype ANP32B.

Influenza A virus replication is attenuated in a monoclonal mutant cell line

To further probe the potential significance of the ANP32B-D130A variant, we generated the homozygous wildtype *Anp32A* / mutant *Anp32B* genotype by CRISPR/Cas9 genome editing in eHAP cells. Using a human codon-optimized DNA endonuclease SpCas9 and a single-stranded DNA homology-directed repair (HDR) template to introduce the point mutation, we obtained a monoclonal cell line carrying the desired genotype (Supplementary Figure 3A-C). We selected an unsuccessfully edited clone to serve as a negative control, and carried out Western blotting analysis to ensure wildtype ANP32A and mutant ANP32B were expressed in control and mutant cells (Supplementary Figure 3D). Using minigenome reporter assays, we found that reconstituted polymerases from H3N2 Vic/75 and pH1N1 Eng/195 were less active in edited cells expressing wildtype ANP32A and ANP32B-D130A (Figure 4A and B). This was not due to differential expression of transfected RNP components (Figure 4C).

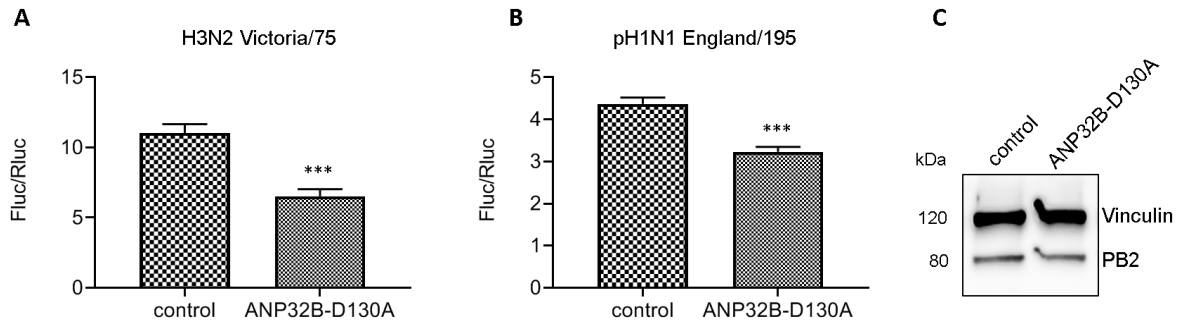

Figure 4 FluPol activity is attenuated in ANP32B-D130A mutant cell line *Minigenome reporter assays in monoclonal CRISPR/Cas9-edited cells with H3N2 Victoria (A) and pH1N1 Eng/195 (B) RNP components (PB1, PB2, PA and NP), pPolI-firefly luciferase minigenome reporter, and Renilla luciferase control. Data show mean (SD) of firefly activity normalized to Renilla and analysed by Student t-test from one representative repeat (n = 2 independent triplicate experiments). ***, P < 0.001 (C) Western blot analysis showing Vic/75 FluPol component PB2 expression in control and mutant cells.*

Next we infected mutant and control cells with low-MOI (0.005) recombinant influenza A viruses containing internal genes from H3N2 Vic/75 and pH1N1 Eng/195 viruses, with the

neuraminidase (NA) and haemagglutinin (HA) external genes of the laboratory-adapted H1N1 PR/8 virus. In addition, we infected eHAP cells lacking ANP32B (BKO). Influenza A virus replication was severely attenuated in mutant cells, in comparison with either control or BKO cells, in particular at early time points. H3N2 Vic/75 infectious virus production in mutant cells was almost 100-fold lower than in control cells at 16h and 24h post-infection (Figure 5A). This difference was even more pronounced in cells infected with pH1N1 Eng/195 virus, which at 24h and 48h post-infection is approximately 1000-fold less productive in mutant cells (Figure 5B). Both viruses replicated to higher titres in cells that completely lack ANP32B (BKO) than in cells expressing the ANP32B-D130A mutant.

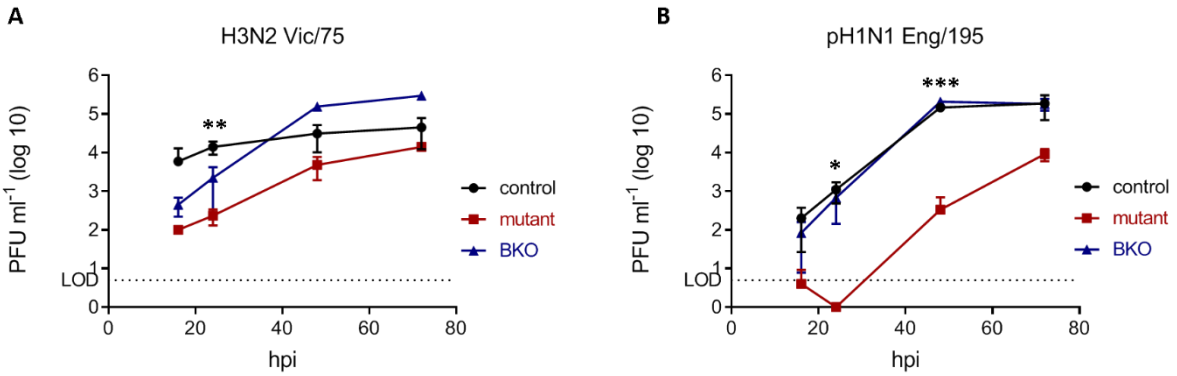

Figure 5 IAV replication is attenuated in ANP32B-D130A mutant cells *Control (black), mutant (red), and BKO (blue) monoclonal cells were infected with H3N2 Victoria/75 (A) or pH1N1 England/195 (B) 6:2 reassortant viruses with PR8 hemagglutinin (HA) and neuraminidase (NA) genes at MOI = 0.005 and incubated at 37 ^{0}C in the presence of 1 µg/ml trypsin to allow multicycle replication. Supernatants were harvested at the indicated times post-infection and pfu/ml established by plaque assay on MDCK cells. LOD (dotted line) denotes the limit of detection in plaque assays. Shown are representative data from one of two independent infection experiments carried out in triplicate. P values were calculated per time point by student's t test and represent differences between control and mutant cell lines. *P<0.05; **P<0.01; ***P<0.01*

DISCUSSION

Here, we used publicly available databases to perform a biased screen for naturally occurring single nucleotide variants in human *Anp32A* and *Anp32B*, under the hypothesis that some mutations may affect susceptibility to influenza virus infection. One of the mutations, which translates to an aberrant ANP32B-D130A protein, is highly enriched in carriers of Latino descent. Although most carriers of the SNV will be heterozygous for the mutation, 25 homozygotes are reported in the gnomAD database. We generated this naturally occurring homozygous genotype by CRISPR/Cas9 genome editing in low-ploidy human eHAP cells, and found that IAV FluPol activity and virus replication were significantly attenuated in the mutant cell line, compared to wildtype control cells or cells lacking ANP32B. Thus we have provided the first example of a single nucleotide variant in the coding region of a human gene that might confer some protection against influenza virus infection. The nucleotide substitution, an A>C transversion in exon 4 of the *Anp32B* gene, gives rise to a protein product bearing an alanine residue at position 130, in lieu of the canonical aspartate (ANP32B-D130A). This substitution entails a loss of a negatively charged amino acid with the potential to form a salt bridge or hydrogen bond with a potential binding partner. Indeed, using a split luciferase assay, we show reduced interaction of ANP32B-D130A with IAV polymerase.

Although we and others have previously reported redundancy in reconstituted systems for ANP32A and B in their support of FluPol activity (Staller et al., 2019; Zhang et al., 2019), the data presented here implies that deleterious mutations in one ANP32 protein might exert dominant negative effects on the pro-viral activity of the other. The mechanism behind the dominant negative effect cannot be readily explained by the split luciferase assay we used here that indicates that the D130A mutation weakens the interaction between ANP32B and FluPol. Further studies to elucidate the binding interfaces and valency of this virus-host interaction will be required to account for our findings.

In addition, it is important to bear in mind that the outcome of genetic variation will also depend on gene dosing in relevant tissues. The genotype-tissue expression (GTEx) portal uses whole genome sequencing and RNA-Seq data to estimate gene expression in 54 non-diseased human tissue types from nearly 1,000 individuals (Lonsdale et al., 2013). ANP32A and ANP32B are both clearly detectable in healthy lung tissue, at a median transcripts per kilobase million (TPM) of 42 and 201, respectively. There are thus 4.8-fold more ANP32B transcripts than ANP32A transcripts in the lung, suggesting that mutations that impair that pro-viral function of ANP32B such as ANP32B-D130A might have significant effects on virus replication in the major target tissue.

A caveat of the work here presented is the use of human eHAP cells where (primary) respiratory epithelium would have been preferable. We selected eHAP cells for their low ploidy, which renders CRISPR/Cas9 genome editing more straightforward. More commonly used laboratory cell lines like A549 or HEK-293 derivatives are polyploid (Giard et al., 1973; Graham et al., 1977; Lin et al., 2014). We have shown previously that eHAP cells are a suitable model for influenza virus infection (Long et al., 2019; Mistry et al., 2020; Peacock et al., 2020; Staller et al., 2019). A drawback of using a haploid cell line is that heterozygous genotypes cannot be generated. Thus far we have been unable to trace carriers of the variants but future work using diploid epithelial cells that reflect the heterozygous genotype could indicate whether heterozygotes are also likely to display reduced influenza susceptibility.

In conclusion, we have provided the first example of a single nucleotide variant in the coding region of a human gene that may offer carriers some protection against influenza virus. This work has the potential to help elucidate the mechanism through which ANP32 proteins support influenza virus replication, and can inform future intervention.

ACKNOWLEDGEMENTS

The authors wish to thank David Gaboriau for help with microscopy, and the St. Mary's NHLI FACS core facility for support, instrumentation, and help with single cell sorting. The Facility for Imaging by Light Microscopy (FILM) at Imperial College London is partially supported by funding from the Wellcome Trust (grant 104931/Z/14/Z) and BBSRC (grant BB/L015129/1)

E.S. was supported by an Imperial College President's Scholarship. L.B. was supported by Wellcome Trust grant 209213/Z/17/Z. R.F. was supported by Wellcome Trust grant 200187/Z/15/Z. T.P.P. was supported by BBSRC grant BB/R013071/1. V.S.S. was supported by UKRI Future Leaders Fellowship MR/S032304/1. C.M.S. and W.S.B. were funded by Wellcome Trust grant 205100 and BBSRC grant BB/K002456/1.

AUTHOR CONTRIBUTIONS

Conceptualization, E.S. and W.S.B.; Methodology, E.S., C.M.S., V.S.S., and W.S.B.; Investigation, E.S., L.B., and R.F.; Resources, T.P.P.; Writing – Original Draft, E.S.; Writing – Review and Editing, all authors; Visualization, E.S. and C.M.S.; Supervision, C.M.S, V.S.S., and W.S.B.; Funding Acquisition, W.S.B.

DECLARATION OF INTERESTS

The authors declare no competing interests.

EXPERIMENTAL PROCEDURES

Cell culture

Human eHAP cells (Horizon Discovery) were cultured in Iscove's modified Dulbecco's medium (IMDM; Thermo Fisher) supplemented with 10% fetal bovine serum (FBS; Labtech), 1% nonessential amino acids (NEAA; Gibco), and 1% penicillin/streptomycin (Invitrogen). Human embryonic kidney (293T) cells (ATCC) and Madin-Darby canine kidney (MDCK) cells (ATCC) were maintained in Dulbecco's modified Eagle's medium (DMEM; Invitrogen) supplemented with 10% FBS, 1% NEAAs, and 1% penicillin/streptomycin. All cells were maintained at 37°C in a 5% CO^2 atmosphere.

Plasmids and cloning

Human FLAG-tagged pCAGGS-ANP32A and ANP32B expression plasmids have been described (Staller et al., 2019). Mutant proteins were cloned from these plasmids by overlapping touchdown PCR, using primers CCAACCTGAATAACTACCGCGAGAAC and GTTCTCGCGGTAGTTATTCAGGTTGG (ANP32A-D130N), GAATGACTACCAAGAGAACGTGTTC and GAACACGTTCTCTTGGTAGTCATTC (ANP32A-R132Q), GAGGCCCCTGATGCTGACGCCGAGG and CCTCGGCGTCAGCATCAGGGGCCTC (ANP32A-S158A), GAGGCCCCTGATACTGACGCCGAGGGC and GCCCTCGGCGTCAGTATCAGGGGCCTC (ANP32A-S158T), GTGACAAACGTGAATGACTATCGG and CCGATAGTCATTCACGTTTGTCAC (ANP32B-L128V), CAAACCTGAATGCCTATCGGGAGAGC and GCTCTCCCGATAGGCATTCAGGTTTG (ANP32B-D130A), GACTATCGGCAGAGCGTGTTTAAG and CTTAAACACGCTCTGCCGATAGTC (ANP32B-E133Q), GAGAGCGTGTTTAAGCACCTGCCACAGCTG and CAGCTGTGGCAGGTGCTTAAACACGCTCTC (ANP32B-L138H), GTTGCTGCCACAGTTTACTTATCTCGA and TCGAGATAAGTAAACTGTGGCAGCAAC (ANP32B-L142F). Expression plasmids encoding H3N2 Vic/75 and pH1N1 RNP components PB1, PB2, PA and NP have been described (Staller et al., 2019), as have pCAGGS-ANP32A$_{luc2C}$, pCAGGS-luc1, pCAGGS-luc2, and H5N1 50-92 PB1$_{luc1C}$ (Long et al., 2019; Mistry et al., 2020). pPolI reporter plasmid containing firefly luciferase flanked by IAV-specific promoters, and pCAGGS-*Renilla* luciferase transfection / cellular transcription control have been previously described (Staller et al., 2019). Expression plasmids pCAGGS-ANP32B$_{luc2C}$, ANP32A-D130N$_{luc2C}$, ANP32B-L128V$_{luc2C}$, and ANP32B-D130A$_{luc2C}$ were cloned by overlapping touchdown PCR. All plasmid constructs were verified by Sanger sequencing and analyzed in Geneious prime 2019.

CRISPR/Cas9 genome editing

Guide RNA GCACTCTCTCGGTAGTCATTC was designed manually against the protospacer sequence in exon 4 of *Anp32B* to target DNA endonuclease SpCas9, expressed from Addgene plasmid # 62988 (PX459), to the target nucleotide (Supplementary Figure 3A). The guide RNA itself was cloned into Addgene plasmid # 80457 (pmCherry_gRNA). A custom-designed 88 base ssODN (single strand DNA) homology-directed repair template, harbouring the point mutation (cytosine in bold) and a silent PAM mutation (thymidine in italic script) – GAAAAGCCTGGACCTCTTTAACTGTGAGGTTACCAA*T*CTGAATG**C**CTACCGAGAGAGTG TCTTCAAGCTCCTGCCCCAGCTTACCTAC – was obtained from Integrated DNA Technologies (IDT). Equal amounts of PX459 and pmCherry_gRNA (total 1 µg), and 1.0 µl 10 µM ssODN template, were transfected by electroporation into approximately 400,000 eHAP cells using the Neon™ transfection system (Invitrogen). Cells and DNA were mixed into a 10 µl volume of suspension buffer, which was subjected to a single 1,200 Volt pulse for a duration of 40 ms. Cells were incubated at 37^0C for 24 hours in IMDM growth medium without antibiotics. A fluorescence-activated cell sorter (FACS) Aria IIIU (BD Biosciences) with an 85-µm nozzle was used to sort cells expressing mCherry (550-650 nm emission) into 96-well plates containing growth medium. Single cells were grown out into monoclonal populations over a period of 10 to 14 days. Total genomic DNA was extracted using the Purelink™ Genomic DNA Mini Kit (Invitrogen) and amplified by touchdown PCR to generate a 1,561-base pair fragment of the edited locus (primers TACCTCTGCCCTCTCAATCTCT and ACGCACACAAACACACACTATT). PCR products were then incubated at 65^0C for 30 minutes in the presence of BsmI restriction enzyme (NEB). The resulting DNA fragments were separated by 1.5% agarose gel electrophoresis. Potentially successfully edited clones were verified by Sanger sequencing (primers TAAAGACCGCTTGATACCCAGG and TGAGGCTGAGTGGGTAGTGG), and analysed in Geneious prime 2019.

Minigenome reporter assays

In order to measure influenza virus polymerase activity, pCAGGS expression plasmids encoding H3N2 Vic/75 or pH1N1 Eng/195 PB1 (0.02 µg), PB2 (0.02 µg), PA (0.01 µg), and NP (0.04 µg) were transfected into 100,000 eHAP cells using Lipofectamine 3000 (Thermo Fisher) at ratios of 2 µl P3000 reagent and 3 µl Lipofectamine 3000 reagent per µg plasmid DNA. As a reporter construct, we transfected 0.02 µg pPolI-luc, which encodes a minigenome containing a firefly luciferase reporter flanked by influenza A virus promoter sequences. pCAGGS-*Renilla* luciferase (0.02 µg) was co-transfected as a transfection and toxicity control. 0.04 micrograms of the indicated ANP32-FLAG constructs was co-expressed to determine their effect on polymerase activity. Twenty-four hours after transfection, cells were lysed in 50 µl passive lysis buffer (Promega) for 30 minutes at room temperature with gentle shaking. Bioluminescence generated by firefly and *Renilla* luciferases was measured using the dual-luciferase system (Promega) on a FLUOstar Omega plate reader (BMG Labtech).

Split luciferase complementation assay

pCAGGS expression plasmids encoding H5N1 50-92 or H3N2 Vic/75 $PB1_{luc1C}$, PB2-627K, PA, and the relevant $ANP32_{luc2C}$ construct were transfected into 100,000 293T cells at a ratio of 1:1:1:1 (15 ng per well). Control conditions contained pCAGGS-luc1 and untagged PB1, or pCAGGS-luc2 and untagged ANP32A, respectively, with all other components remaining constant. Empty pCAGGS plasmid was used to ensure total transfected DNA was equal

across conditions. Twenty-four hours after transfection, cells were lysed in 50 µl *Renilla* lysis buffer (Promega) for 1 h at room temperature with gentle shaking (*Gaussia* and *Renilla* luciferase share the same substrate). Bioluminescence generated by *Gaussia* luciferase was measured using the Renilla luciferase kit (Promega) on a FLUOstar Omega plate reader (BMG Labtech). Normalized luminescence ratios (NLR) were calculated by dividing the signal from the potential interacting partners by the sum of the two controls, as described (Mistry et al., 2020).

Western blotting

At least 250,000 cells were lysed in buffer containing 50 mM Tris-HCl (pH 7.8; Sigma-Aldrich), 100 mM NaCl, 50 mM KCl, and 0.5% Triton X-100 (Sigma-Aldrich), supplemented with a cOmplete EDTA-free protease inhibitor cocktail tablet (Roche) and prepared in Laemmli 4x buffer (Bio-Rad) after protein concentration had been established by spectrophotometry (DeNovix DS-11 FX+ spectrophotometer). Equal amounts of total protein (20-50 µg per lane) was resolved by SDS-PAGE using Mini Protean TGX precast gels 4% to 20% (Bio-Rad). Immunoblotting by semi-dry transfer (Bio-Rad Trans-Blot SD semidry transfer cell) onto nitrocellulose membranes (Amersham Protran Premium 0.2 µm NC; GE Healthcare) was carried out using the following primary antibodies: rabbit α-vinculin (catalog number ab129002, 1/1,000; Abcam), rabbit α-ANP32A (catalog number ab51013, 1/500; Abcam), rabbit α-ANP32B (10843-1-AP, 1/1,000; Proteintech), mouse α-FLAG (catalog number F1804, 1/500; Sigma-Aldrich) and rabbit α-IAV PB2 (catalog number GTX125926, 1/2,000; GeneTex). The following secondary antibodies were used: sheep α-rabbit horseradish peroxidase (HRP) (catalog number AP510P, 1/10,000; Merck) and goat α-mouse HRP (STAR117P, 1/5,000; AbD Serotec). Protein bands were visualized by chemiluminescence using SuperSignal™ West Femto substrate (Thermofisher Scientific) on a Fusion-FX imaging system (Vilber Lourmat).

Immunofluorescence microscopy

Approximately 100,000 eHAP cells were cultured on sterilised glass coverslips and transfected as per minigenome reporter assay protocol. Twenty-four hours after transfection, cells were fixed in 4% paraformaldehyde and permeabilized in 0.2% Triton X-100. FLAG-tagged ANP32 constructs were visualised with primary antibody mouse α-FLAG (F1804; 1/200; Sigma) for 2 hours at 37^{0}C in a humidified chamber. Cells were incubated with secondary antibody goat α-mouse Alexa Fluor-568 (1/200; Life Technologies) for 1 hour at 37^{0}C in a humidified chamber, and counterstained with DAPI. Coverslips were mounted on glass slides using Vectashield mounting medium (H-1000-10; Vector Laboratories). Cells were imaged with a Zeiss Cell Observer widefield microscope with ZEN Blue software, using a Plan-Apochromat x100 1.40-numerical aperture oil objective (Zeiss), an Orca-Flash 4.0 complementary metal-oxide semiconductor (CMOS) camera (frame, 2,048 x 2,048 pixels; Hamamatsu), giving a pixel size of 65 nm, and a Colibri 7 light source (Zeiss). Channels acquired and filters for excitation and emission were 4',6-diamidino-2- phenylindole (DAPI) (excitation [ex], 365/12 nm, emission [em] 447/60 nm), and TexasRed (ex 562/40 nm, em 624/40 nm). All images were analyzed and prepared with Fiji software.

Influenza virus infection

500,000 CRISPR/Cas9-modified monoclonal eHAP cells were infected with ~2,500 plaque-forming units (PFU) H3N2 Vic/75 6:2 or pH1N1 Eng/195 6:2 virus diluted in 200 µl serum-free IMDM for 1 hour at 37°C (MOI 0.005) to allow virus to adsorb and enter the cells. The inoculum was removed and cells were incubated in room-temperature phosphate-buffered saline / HCl at pH 3.0 for 3 minutes to inactivate residual virus. Cells were incubated at 37°C

in serum-free cell culture medium (IMDM) supplemented with 1 µg/ml L-1-tosylamide-2-phenylethyl chloromethyl ketone (TPCK) trypsin (Worthington-Biochemical). Cell supernatants were harvested at indicated time points post-infection. Infectious titres were determined by plaque assay on MDCK cells. Virus infection assays were performed in triplicate on two separate occasions.

Safety/biosecurity

All work with infectious agents was conducted in biosafety level 2 facilities, approved by the Health and Safety Executive of the United Kingdom and in accordance with local rules, at Imperial College London, United Kingdom.

Structural modelling

Structural models of ANP32A and B were created using iTASSER structural prediction software (based primarily on huANP32B [GenBank accession number 2RR6A] and huANP32A [accession number 2JQDA], and 2JEOA). The three-dimensional structural models were visualized and created in UCSF Chimera. Amino acid residues affected by selected SNVs are highlighted in purple (ANP32A) or blue (ANP32B) stick format.

Bioinformatics

Human genomic information was obtained using the following publicly available databases: gnomAD (https://gnomad.broadinstitute.org/); NCBI dbSNP (https://www.ncbi.nlm.nih.gov/snp/); ALSPAC (http://www.bristol.ac.uk/alspac/); TOPMed (https://www.nhlbiwgs.org/); 1000G (https://www.internationalgenome.org/); GO-ESP (https://esp.gs.washington.edu/drupal/)

REFERENCES

.

Beck, S., Zickler, M., Pinho dos Reis, V., Günther, T., Grundhoff, A., Reilly, P.T., Mak, T.W., Stanelle-Bertram, S., and Gabriel, G. (2020). ANP32B Deficiency Protects Mice From Lethal Influenza A Virus Challenge by Dampening the Host Immune Response. Frontiers in Immunology *11*.

Carette, J.E., Raaben, M., Wong, A.C., Herbert, A.S., Obernosterer, G., Mulherkar, N., Kuehne, A.I., Kranzusch, P.J., Griffin, A.M., and Ruthel, G. (2011). Ebola virus entry requires the cholesterol transporter Niemann–Pick C1. Nature *477*, 340-343.

Carrington, M., Dean, M., Martin, M.P., and O'Brien, S.J. (1999). Genetics of HIV-1 Infection: Chemokine Receptor Ccr5 Polymorphism and Its Consequences. Human Molecular Genetics *8*, 1939-1945.

Cassonnet, P., Rolloy, C., Neveu, G., Vidalain, P.O., Chantier, T., Pellet, J., Jones, L., Muller, M., Demeret, C., Gaud, G.*, et al.* (2011). Benchmarking a luciferase complementation assay for detecting protein complexes. Nature methods *8*, 990-992.

Chen, Y., Zhou, J., Cheng, Z., Yang, S., Chu, H., Fan, Y., Li, C., Wong, B.H., Zheng, S., Zhu, Y.*, et al.* (2015). Functional variants regulating LGALS1 (Galectin 1) expression affect human susceptibility to influenza A(H7N9). Scientific reports *5*, 8517.

Ciancanelli, M.J., Abel, L., Zhang, S.Y., and Casanova, J.L. (2016). Host genetics of severe influenza: from mouse Mx1 to human IRF7. Current opinion in immunology *38*, 109-120.

Essletzbichler, P., Konopka, T., Santoro, F., Chen, D., Gapp, B.V., Kralovics, R., Brummelkamp, T.R., Nijman, S.M., and Burckstummer, T. (2014). Megabase-scale deletion using CRISPR/Cas9 to generate a fully haploid human cell line. Genome research *24*, 2059-2065.

485 Everitt, A.R., Clare, S., Pertel, T., John, S.P., Wash, R.S., Smith, S.E., Chin, C.R., Feeley, E.M., Sims, J.S.,
486 Adams, D.J*., et al.* (2012). IFITM3 restricts the morbidity and mortality associated with influenza.
487 Nature *484*, 519-523.
488 Fu, W., O'Connor, T.D., Jun, G., Kang, H.M., Abecasis, G., Leal, S.M., Gabriel, S., Rieder, M.J.,
489 Altshuler, D., Shendure, J*., et al.* (2013). Analysis of 6,515 exomes reveals the recent origin of most
490 human protein-coding variants. Nature *493*, 216-220.
491 Genomes Project, C., Auton, A., Brooks, L.D., Durbin, R.M., Garrison, E.P., Kang, H.M., Korbel, J.O.,
492 Marchini, J.L., McCarthy, S., McVean, G.A*., et al.* (2015). A global reference for human genetic
493 variation. Nature *526*, 68-74.
494 Giard, D.J., Aaronson, S.A., Todaro, G.J., Arnstein, P., Kersey, J.H., Dosik, H., and Parks, W.P. (1973).
495 In vitro cultivation of human tumors: establishment of cell lines derived from a series of solid
496 tumors. Journal of the National Cancer Institute *51*, 1417-1423.
497 Graham, F.L., Smiley, J., Russell, W.C., and Nairn, R. (1977). Characteristics of a human cell line
498 transformed by DNA from human adenovirus type 5. The Journal of general virology *36*, 59-74.
499 Hong, R., Macfarlan, T., Kutney, S.N., Seo, S.-b., Mukai, Y., Yelin, F., Pasternack, G.R., and Chakravarti,
500 D. (2004). The Identification of Phosphorylation Sites of pp32 and Biochemical Purification of a
501 Cellular pp32-kinase. Biochemistry *43*, 10157-10165.
502 Huyton, T., and Wolberger, C. (2007). The crystal structure of the tumor suppressor protein pp32
503 (Anp32a): structural insights into Anp32 family of proteins. Protein science : a publication of the
504 Protein Society *16*, 1308-1315.
505 Karczewski, K.J., Francioli, L.C., Tiao, G., Cummings, B.B., Alföldi, J., Wang, Q., Collins, R.L., Laricchia,
506 K.M., Ganna, A., Birnbaum, D.P*., et al.* (2019). Variation across 141,456 human exomes and genomes
507 reveals the spectrum of loss-of-function intolerance across human protein-coding genes. bioRxiv,
508 531210.
509 Karlsson, E.K., Kwiatkowski, D.P., and Sabeti, P.C. (2014). Natural selection and infectious disease in
510 human populations. Nature Reviews Genetics *15*, 379-393.
511 Kondoh, T., Letko, M., Munster, V.J., Manzoor, R., Maruyama, J., Furuyama, W., Miyamoto, H.,
512 Shigeno, A., Fujikura, D., Takadate, Y*., et al.* (2018). Single-Nucleotide Polymorphisms in Human
513 NPC1 Influence Filovirus Entry Into Cells. The Journal of infectious diseases *218*, S397-s402.
514 Lin, Y.C., Boone, M., Meuris, L., Lemmens, I., Van Roy, N., Soete, A., Reumers, J., Moisse, M.,
515 Plaisance, S., Drmanac, R*., et al.* (2014). Genome dynamics of the human embryonic kidney 293
516 lineage in response to cell biology manipulations. Nat Commun *5*, 4767.
517 Lindesmith, L., Moe, C., Marionneau, S., Ruvoen, N., Jiang, X., Lindblad, L., Stewart, P., LePendu, J.,
518 and Baric, R. (2003). Human susceptibility and resistance to Norwalk virus infection. Nature medicine
519 *9*, 548-553.
520 Long, J.S., Giotis, E.S., Moncorge, O., Frise, R., Mistry, B., James, J., Morisson, M., Iqbal, M., Vignal, A.,
521 Skinner, M.A*., et al.* (2016). Species difference in ANP32A underlies influenza A virus polymerase
522 host restriction. Nature *529*, 101-104.
523 Long, J.S., Idoko-Akoh, A., Mistry, B., Goldhill, D., Staller, E., Schreyer, J., Ross, C., Goodbourn, S.,
524 Shelton, H., Skinner, M.A*., et al.* (2019). Species specific differences in use of ANP32 proteins by
525 influenza A virus. eLife *8*, e45066.
526 Lonsdale, J., Thomas, J., Salvatore, M., Phillips, R., Lo, E., Shad, S., Hasz, R., Walters, G., Garcia, F.,
527 Young, N*., et al.* (2013). The Genotype-Tissue Expression (GTEx) project. Nature Genetics *45*, 580-
528 585.
529 Mistry, B., Long, J.S., Schreyer, J., Staller, E., Sanchez-David, R.Y., and Barclay, W.S. (2020).
530 Elucidating the Interactions between Influenza Virus Polymerase and Host Factor ANP32A. Journal of
531 virology *94*, e01353-01319.
532 Peacock, T.P., Sheppard, C.M., Staller, E., and Barclay, W.S. (2019). Host Determinants of Influenza
533 RNA Synthesis. Annual Review of Virology *6*, 215-233.

534 Peacock, T.P., Swann, O.C., Staller, E., Leung, P.B., Goldhill, D.H., Zhou, H., Long, J.S., and Barclay,
535 W.S. (2020). Swine ANP32A supports avian influenza virus polymerase. bioRxiv,
536 2020.2001.2024.916916.
537 Pittman, K.J., Glover, L.C., Wang, L., and Ko, D.C. (2016). The legacy of past pandemics: common
538 human mutations that protect against infectious disease. PLoS pathogens *12*.
539 Prabhu, S.S., Chakraborty, T.T., Kumar, N., and Banerjee, I. (2018). Association between IFITM3
540 rs12252 polymorphism and influenza susceptibility and severity: A meta-analysis. Gene *674*, 70-79.
541 Reilly, P.T., Yu, Y., Hamiche, A., and Wang, L. (2014). Cracking the ANP32 whips: important functions,
542 unequal requirement, and hints at disease implications. BioEssays : news and reviews in molecular,
543 cellular and developmental biology *36*, 1062-1071.
544 Sherry, S.T., Ward, M.H., Kholodov, M., Baker, J., Phan, L., Smigielski, E.M., and Sirotkin, K. (2001).
545 dbSNP: the NCBI database of genetic variation. Nucleic acids research *29*, 308-311.
546 Staller, E., Sheppard, C.M., Neasham, P.J., Mistry, B., Peacock, T.P., Goldhill, D.H., Long, J.S., and
547 Barclay, W.S. (2019). ANP32 Proteins Are Essential for Influenza Virus Replication in Human Cells.
548 Journal of virology *93*.
549 Taliun, D., Harris, D.N., Kessler, M.D., Carlson, J., Szpiech, Z.A., Torres, R., Taliun, S.A.G., Corvelo, A.,
550 Gogarten, S.M., Kang, H.M*., et al.* (2019). Sequencing of 53,831 diverse genomes from the NHLBI
551 TOPMed Program. bioRxiv, 563866.
552 Te Velthuis, A.J., and Fodor, E. (2016). Influenza virus RNA polymerase: insights into the mechanisms
553 of viral RNA synthesis. Nature reviews Microbiology *14*, 479-493.
554 Thorven, M., Grahn, A., Hedlund, K.-O., Johansson, H., Wahlfrid, C., Larson, G., and Svensson, L.
555 (2005). A Homozygous Nonsense Mutation (428G→A) in the Human Secretor (FUT2)
556 Gene Provides Resistance to Symptomatic Norovirus (GGII) Infections. Journal of virology *79*, 15351-
557 15355.
558 Tochio, N., Umehara, T., Munemasa, Y., Suzuki, T., Sato, S., Tsuda, K., Koshiba, S., Kigawa, T., Nagai,
559 R., and Yokoyama, S. (2010). Solution structure of histone chaperone ANP32B: interaction with core
560 histones H3-H4 through its acidic concave domain. Journal of molecular biology *401*, 97-114.
561 Walter, K., Min, J.L., Huang, J., Crooks, L., Memari, Y., McCarthy, S., Perry, J.R., Xu, C., Futema, M.,
562 Lawson, D*., et al.* (2015). The UK10K project identifies rare variants in health and disease. Nature
563 *526*, 82-90.
564 Zhang, H., Zhang, Z., Wang, Y., Wang, M., Wang, X., Zhang, X., Ji, S., Du, C., Chen, H., and Wang, X.
565 (2019). Fundamental Contribution and Host Range Determination of ANP32A and ANP32B in
566 Influenza A Virus Polymerase Activity. Journal of virology *93*.
567 Zhang, Q. (2020). Human genetics of life-threatening influenza pneumonitis. Human genetics.
568 Zhang, Y.-H., Zhao, Y., Li, N., Peng, Y.-C., Giannoulatou, E., Jin, R.-H., Yan, H.-P., Wu, H., Liu, J.-H., Liu,
569 N*., et al.* (2013). Interferon-induced transmembrane protein-3 genetic variant rs12252-C is
570 associated with severe influenza in Chinese individuals. Nature Communications *4*, 1418.
571
572
573

SUPPLEMENTARY FIGURES

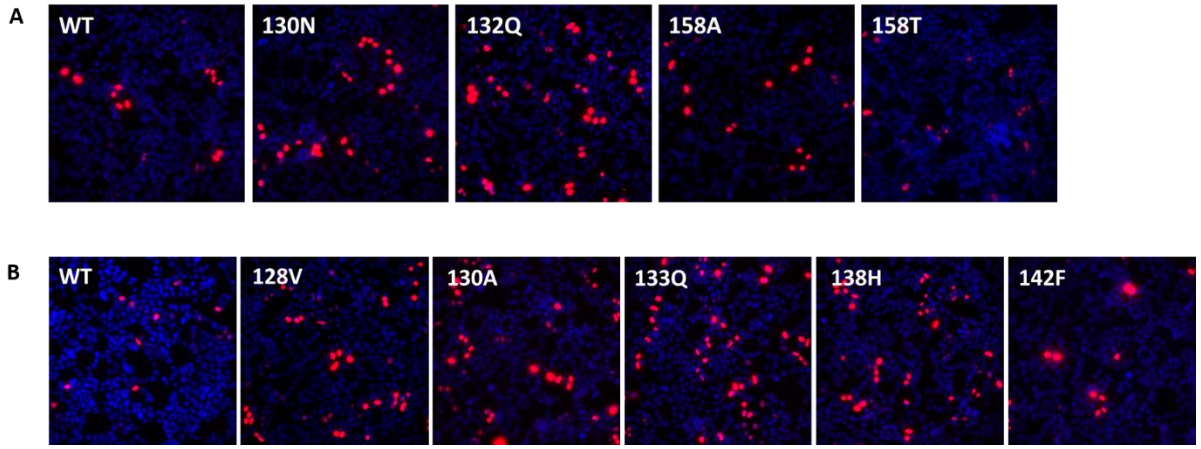

Supplementary Figure 1. Mutant ANP32 proteins localise to the cell nucleus
Immunofluorescence analysis showing nuclear localisation of mutant FLAG-tagged ANP32A (A) or ANP32B (B) proteins, detected with anti-FLAG primary antibody and Alexa Fluor-568 anti-mouse conjugate and counterstained with DAPI

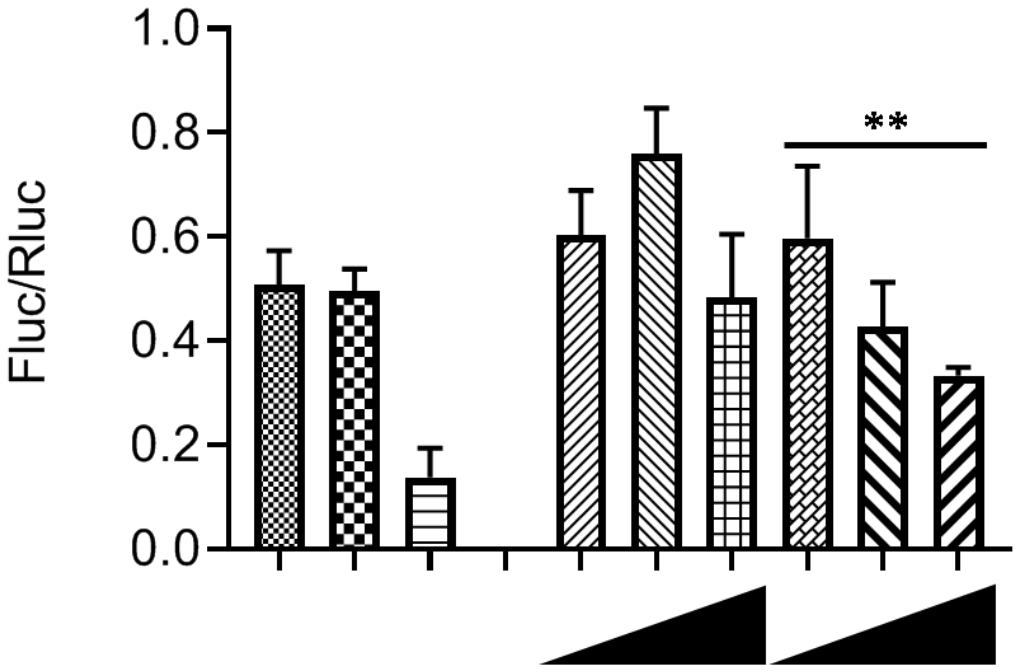

Plasmid	A	B	C	D	E	F	G	H	I	J
WT ANP32A	10				10	10	10	10	10	10
WT ANP32B		10			1	5	10			
ANP32B-D130A			10					1	5	10
Empty	10	10	10	20	9	5		9	5	

Supplementary Figure 2 ANP32B-D130A exerts a dominant negative effect over ANP32A
Minigenome reporter assay in approximately 100,000 dKO cells with reconstituted pH1N1 Eng/195 RNP components (PB1, PB2, PA and NP), pPolI-firefly luciferase minigenome reporter, and Renilla control. Conditions contain indicated amounts (in ng) of co-transfected FLAG-tagged pCAGGS-

*ANP32A (WT ANP32A), ANP32B (WT ANP32B) or ANP32B-D130A. Empty pCAGGS was used to make sure equal amounts of total DNA were transfected across conditions. Data show mean (SD) of firefly activity normalized to Renilla and analysed by one-way ANOVA. **, P < 0.01.*

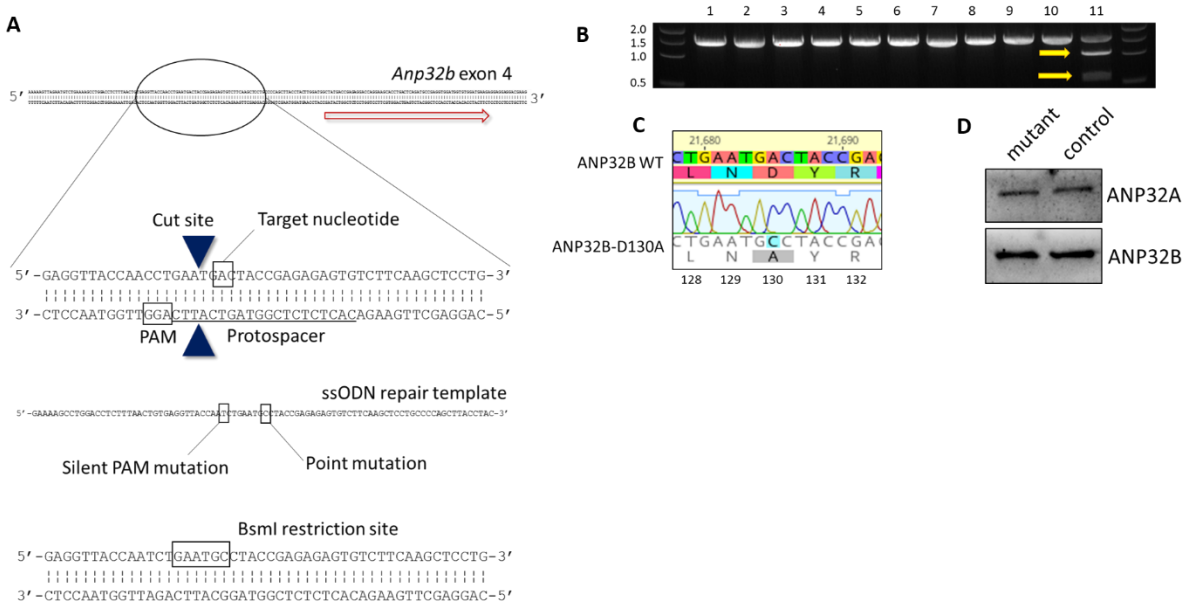

Supplementary Figure 3 Generation of naturally occurring mutant genotype by genome editing *(A) Anp32B is located on Chromosome 9, with the codon encoding 130D in exon 4 of the gene. The red arrow indicates the reading direction. A protospacer-adjacent motif (PAM) was identified near the target adenine on the opposite DNA strand, and a guide RNA was designed against the protospacer (underlined). SpCas9 cut two base pairs upstream of the target nucleotide (dark blue arrowheads). An 88-base single-stranded DNA (ssODN) homology-directed repair (HDR) template was designed bearing the missense A>C substitution as well as a silent PAM mutation between homology arms. A successful edit introduced a BsmI restriction site (GAATGC) not present in the wildtype allele, enabling screening by PCR amplification of a 1,561 base pair genome fragment followed by restriction digestion of the PCR product (B). A successfully edited allele is cleaved into 1,008 and 553 base pair DNA fragments. Potentially positive clones were verified by Sanger sequencing (C). (D) Western blotting analysis with specific antibodies against ANP32A and ANP32B in a mutant and control monoclonal cell line shows equal expression of both proteins.*